J. Fluid Mech. (1992), *vol.* 241, *pp.* 349–369
Printed in Great Britain

Jump conditions across normal shock waves in pure vapour–droplet flows

By A. GUHA
Whittle Laboratory, University of Cambridge, Madingley Road, Cambridge CB3 0DY, UK

(Received 11 December 1990 and in revised form 16 January 1992)

Closed-form analytical jump conditions across normal shock waves in pure vapour–droplet flows have been derived for different boundary conditions. They are equally applicable to partly and fully dispersed shock waves. Collectively they may be called the generalized Rankine–Hugoniot relations for wet vapour. A phase diagram is constructed which specifies the type of shock structure obtained in vapour–droplet flow given some overall parameters. It is shown that in addition to the partly and fully dispersed shock waves that are possible in any relaxing medium, there also exists a class of shock waves in wet vapour in which the two-phase relaxing medium reverts to a single-phase non-relaxing one. An analytical expression for the limiting upstream wetness fraction below which complete evaporation will take place inside a shock of specified strength has been deduced. A new theory has been formulated which shows that, depending on the upstream wetness fraction, a continuous transition exists for the shock velocity between its frozen and fully equilibrium values. The mechanisms of entropy production inside a shock are also discussed.

1. Introduction

A pure vapour–droplet mixture is a relaxing medium and accordingly exhibits the property of frequency dispersion, i.e. the speed of an harmonic sound wave through the medium is a function of the frequency itself. If the frequency is very high, the sound wave travels through the medium such that all relaxation processes arising out of non-equilibrium mass, momentum and energy transfer between the two phases remain essentially frozen. The medium behaves like a single-phase vapour and the speed of sound in these situations is termed the frozen speed, a_f. On the other hand, if the frequency of the harmonic sound wave is low, full equilibrium between the vapour and the liquid droplets is maintained always and the wave travels with the equilibrium speed of sound, a_e. The frozen speed is higher than the equilibrium speed and, depending on the frequency, the speed of an harmonic sound wave would vary between these two limits (Becker 1970).

Because of the dispersion in sound speed, two limiting Mach numbers can be defined corresponding to a particular flow velocity V: (i) a frozen Mach number $M_f = V/a_f$, and (ii) an equilibrium Mach number $M_e = V/a_e$. In general $M_e > M_f$. As a result of this, two distinct types of steady shock waves might occur in such a medium, namely a partly dispersed shock where an almost discontinuous wave front (similar to the normal shock wave obtained in a perfect gas) is followed by a long relaxation zone, or a fully dispersed one where flow properties change continuously from one equilibrium state to another. Study of such shock waves is important as they almost invariably occur in the last few stages of low-pressure steam turbines

used for electrical power generation where the flow is transonic with maximum Mach numbers about 2. With growing evidence that a significant amount of 'wetness loss' in turbines operating with wet steam is aerodynamic in origin (and hence controllable by improved design), as opposed to the traditional view of being thermodynamic in nature, it is instructive to study systematically the characteristics of shock waves in isolation before considering their interaction with the aerodynamics of the blade-passage as a whole. (An example of such interaction in convergent–divergent nozzles resulting in oscillating shock waves may be found in Guha & Young 1991.)

The internal structures of fully dispersed and partly dispersed shock waves in pure vapour–droplet flows have been thoroughly discussed by Young & Guha (1991) and Guha (1992) respectively. The development of such shock waves under unsteady situations has been studied by Guha & Young (1989) by analysing the conventional piston-and-cylinder problem in wet vapour. A lucid overview of the complex physics governing shock wave phenomena in vapour–droplet flow may be found in Guha (1991). There are also many references on the structure of other types of dispersed shock waves. For example, Johannesen *et al.* (1962) discussed vibrational relaxation regions in carbon dioxide, Nayfeh (1966) analysed shock structure in a gas containing ablating particles and Rudinger (1964) discussed the same for gas flows carrying small solid particles. The general behaviour of condensing flows was examined by Marble (1969) who discussed the structure of partly dispersed waves, and many non-equilibrium aspects of two-phase, wet steam flow were described by Jackson & Davidson (1983). Measurements of shock propagation in a shock tube have also been performed by Goossens *et al.* (1988) in moist air and by Roth & Fischer (1985) in aerosol droplet evaporation in argon.

This paper concentrates on the relations connecting the end state points of a normal shock wave in pure vapour–droplet mixtures with special reference to wet steam as a particular example. To the best of the author's knowledge, such relations have not been derived before. They may be regarded as the two-phase vapour–droplet-flow counterparts of the Rankine–Hugoniot relations for a perfect gas as discussed in classical gasdynamics. They are equally applicable to partly dispersed or fully dispersed shock waves and although the numerical calculations have been performed here specifically for wet steam, the formulae derived and the conclusions deduced are also valid for other pure vapour–droplet mixtures.

2. Governing equations

The vapour–droplet two-phase medium is considered to be a homogeneous mixture of the continuous vapour phase, at pressure p and temperature T_g, and minute droplets of various sizes. The mixture is assumed to be pure which means that the vapour and liquid phases are of same chemical species. If the volume of the liquid phase is neglected (which is an assumption that restricts the analysis to flows with low wetness fraction, the case of practical importance), the mixture density ρ is related to the vapour density ρ_g via the wetness fraction y and is given by

$$\rho = \rho_g/(1-y). \tag{1}$$

The vapour phase is assumed to behave as a perfect gas with constant specific heat capacities. Thus

$$p = \rho_g R T_g, \tag{2}$$

where R is the specific gas constant. For greater accuracy, more realistic equations of state can be introduced, but these complicate the development and do not provide

further physical insight. Equation (2) implies that the partial pressure due to the liquid droplets is negligible. The thermodynamic equilibrium state is usually specified by the saturation temperature T_s rather than the pressure. The two are related by the Clausius–Clapeyron equation which, for low pressure, is

$$(\mathrm{d}T_s/T_s) = (RT_s/h_{fg})\,(\mathrm{d}p/p), \tag{3}$$

where h_{fg} is the specific enthalpy of evaporation and is a known function of temperature. The mixture enthalpy h is the sum of the contributions from each phase and is given by

$$h = (1-y)\,h_g + yh_l = h_g - yh_{fg}. \tag{4}$$

The subscripts g and l, in this paper, refer to the vapour and liquid phase respectively.

We now consider the structure of stationary, finite-amplitude waves in one-dimensional steady flow. Far upstream of the wave the flow is assumed to be in thermodynamic and inertial equilibrium with a specified pressure and wetness fraction. Far downstream of the wave a new equilibrium condition is re-established. The continuity, momentum and energy equations for the two-phase mixture connecting the two end equilibrium states across a normal shock wave take the form:

continuity $$\rho_1 V_1 = \rho_2 V_2; \tag{5}$$

momentum $$p_1 + \rho_1 V_1^2 = p_2 + \rho_2 V_2^2; \tag{6}$$

energy $$c_p T_{s1} - y_1 h_{fg1} + \tfrac{1}{2}V_1^2 = c_p T_{s2} - y_2 h_{fg2} + \tfrac{1}{2}V_2^2; \tag{7}$$

where c_p is the isobaric specific heat capacity of the vapour phase, V is the common velocity of both phases, ρ is the mixture density and the subscripts 1 and 2 refer to far upstream and far downstream conditions respectively. (The change in enthalpy in the energy equation is obtained from (4).) Note that neither the number of droplets nor their sizes appear in the overall conservation equations. Although they determine the different relaxation timescales and hence, in turn, the thickness of the shock wave, overall changes across the shock wave depend only on the total quantity of the liquid phase present (namely the wetness fraction) and not on its distribution.

Given the upstream condition, the six equations (1)–(3) and (5)–(7) completely specify the downstream state of the shock wave. However, no general analytical solution is possible in this case and the equations have to be solved by an iterative numerical scheme. For moderate strengths of shock waves, it is, however, possible to obtain an approximate analytical solution and this has been derived below. Later it is also shown that if instead of specifying the upstream velocity V_1, the pressure ratio p_2/p_1 across the shock is prescribed a completely general analytical solution of (1)–(7) can be formulated.

3. Approximate Rankine–Hugoniot relations for vapour–droplet mixtures

The ratio of the different flow variables between the two end states of a normal shock wave in an ideal gas can be expressed as functions of the upstream Mach number. They are generally referred to as the Rankine–Hugoniot relations. In the case of a simpler relaxing medium (e.g. solid-particle-laden gas), it can be shown that these relations remain identical (Rudinger 1964) if the upstream equilibrium Mach number (M_{e1}) is used instead of the frozen Mach number (M_{f1}). Derivation of such relations for the case of a shock wave in vapour–droplet mixtures is not straightforward. Difficulties arise mainly because of the mass transfer between the

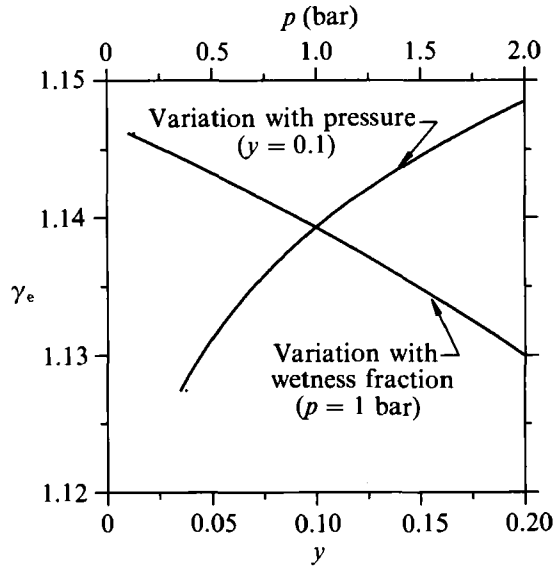

FIGURE 1. Variation of γ_e with wetness fraction y and pressure p.

two phases and also because the pressure and temperature of the vapour–droplet mixture at equilibrium are not independent of each other but are connected via the Clausius–Clapeyron equation.

For deriving the approximate Rankine–Hugoniot relations for weak shock waves where the entropy change is small, we can write the thermodynamic relation for the two-phase mixture as

$$\mathrm{d}h = \mathrm{d}p/\rho, \tag{8}$$

which, after substituting the value of $\mathrm{d}h$ from (4), becomes

$$(1-y)\,c\mathrm{d}T_s - h_{fg}\,\mathrm{d}y = \mathrm{d}p/\rho, \tag{9}$$

where

$$c = c_p + yc_l/(1-y) \tag{10}$$

and c_l is the specific heat capacity of the liquid phase.

With the help of the equation of state, (2), and the Clausius–Clapeyron equation, (3), it may be shown, after considerable algebraic manipulation, that (9) amounts to

$$\mathrm{d}h = \mathrm{d}p/\rho = \frac{\gamma_e}{\gamma_e - 1}\mathrm{d}(p/\rho), \tag{11}$$

where the equilibrium isentropic exponent of the mixture γ_e is given by

$$\gamma_e = \left(1 - \frac{2RT_s}{h_{fg}} + \frac{cT_s}{h_{fg}}\frac{RT_s}{h_{fg}}\right)^{-1}. \tag{12}$$

The value of γ_e is, in general, less than γ, the isentropic exponent for the vapour phase alone. For low-pressure steam, $\gamma \sim 1.32$ and $\gamma_e \sim 1.12$.

Equation (12) shows that γ_e would change slowly with pressure (through saturation temperature T_s) and the wetness fraction (through the mixture specific heat c). Such dependence of γ_e on pressure and wetness fraction has been plotted in figure 1 which shows that unless the change of state is substantial, γ_e can be approximately treated as a constant.

If (11) is integrated between state points 1 and 2, and expanded using (4), assuming γ_e remains constant, then one obtains

$$c_p(T_{s2}-T_{s1})-(y_2 h_{fg2}-y_1 h_{fg1}) = (\gamma_e/(\gamma_e-1))(p_2/\rho_2-p_1/\rho_1). \tag{13}$$

Substitution of (13) in the energy equation (7) results in

$$\frac{\gamma_e}{\gamma_e-1}p_1/\rho_1+\tfrac{1}{2}V_1^2 = \frac{\gamma_e}{\gamma_e-1}p_2/\rho_2+\tfrac{1}{2}V_2^2. \tag{14}$$

Equation (14) is analogous to the energy equation for the adiabatic flow of a single-phase ideal gas. However, in the case of ideal gas, $\mathrm{d}h = c_p\,\mathrm{d}T = \gamma/(\gamma-1)\,\mathrm{d}(p/\rho)$ is a general identity and hence the analogue of (14) is generally valid for any arbitrary adiabatic process in an ideal gas. This may not be the case for two-phase vapour–droplet flow. However, although (14) was derived for an isentropic process, it applies reasonably well across shock waves of low to moderate strength. (This will become evident when calculations based on approximate Rankine–Hugoniot relations are later compared with an exact solution.) One of the conditions, as discussed in §5, for using (14) is that complete evaporation does not occur and this restricts the upper limit of the upstream Mach number to rather low values.

Once the energy equation, (7), has been replaced by (14), the resulting set of equations ((5), (6) and (14)) are identical with the ideal gas analogues, and the Rankine–Hugoniot relations may be derived following the standard procedure given in any gasdynamics textbook. The results are

$$\frac{p_2}{p_1} = \frac{2\gamma_e}{\gamma_e+1}(M_e)_1^2-\frac{\gamma_e-1}{\gamma_e+1}, \tag{15}$$

$$\frac{V_2}{V_1} = \frac{(\gamma_e-1)(M_e)_1^2+2}{(\gamma_e+1)(M_e)_1^2}, \tag{16}$$

$$\rho_2/\rho_1 = V_1/V_2, \tag{17}$$

where the upstream equilibrium Mach number $(M_e)_1$ is given by

$$(M_e)_1 = \frac{V_1}{(a_e)_1} = \frac{V_1}{(\gamma_e p_1/\rho_1)^{\frac{1}{2}}}, \tag{18}$$

where $(a_e)_1$ is the upstream equilibrium speed of sound. (In this paper we use a simpler notation a_e for fully equilibrium speed of sound, since other intermediate speeds of sound are not important here. Thus a_e here corresponds to a_{e3}, for example, in Young & Guha 1991.) The subscripts 1 and 2, as before, refer to the far upstream and far downstream conditions respectively, and ρ is the mixture density.

The temperature ratio across the shock, however, is not given by the perfect gas type Rankine–Hugoniot relation, but must be calculated by integrating the Clausius–Clapeyron equation, (3). Assuming that the value of RT_s/h_{fg} does not change appreciably across the shock wave (which is in keeping with the earlier assumption of constant γ_e), the temperature ratio is approximately

$$T_{s2}/T_{s1} = (p_2/p_1)^{RT_s/h_{fg}}. \tag{19}$$

The downstream wetness fraction can then be calculated from (1) and (2):

$$y_2 = 1-p_2/(R\rho_2 T_{s2}). \tag{20}$$

The range of acceptability of the above equations depends on the validity of (14). (The accuracy of (15)–(18) is compared with an exact solution later in §5.) However,

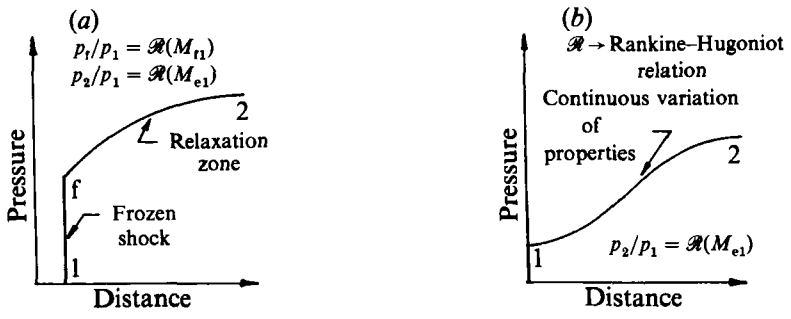

FIGURE 2. Schematic structure of shock waves in a relaxing medium. (*a*) Partly dispersed shock wave, $M_{e1} > 1$, $M_{f1} > 1$. (*b*) Fully dispersed shock wave, $M_{e1} > 1$, $M_{f1} \leqslant 1$.

although not exact, these equations have two advantages: (i) all shock relations could be explicitly written in terms of the upstream parameters only, and (ii) the form of the equations is similar to the well-known Rankine–Hugoniot relations for ideal gas.

It should be noted that (15)–(20) are valid for both partly and fully dispersed shock waves. Partly dispersed shock waves are characterized by an almost discontinuous wave front followed by a relaxation zone and occur when the upstream frozen Mach number is greater than unity ($M_{f1} > 1$, which also implies that $(M_e)_1 > 1$). The overall changes across such a shock wave are given by the above equations while the changes just across the discontinuous wave front are given by the classical Rankine–Hugoniot equation based on M_{f1}. If $M_{f1} < 1$ but $(M_e)_1 > 1$, then a fully dispersed shock wave, which does not have a discontinuous wave front, will appear in the flow field. The above equations again give the overall changes across such waves. Figure 2 schematically depicts the point.

4. A paradox and its solution

If instead of a steady, partly dispersed shock wave sitting at a particular position, one considers the shock wave to be moving with a constant velocity V_s ($= V_1$) through the vapour–droplet mixture initially at rest, then it is easy to show that V_s would be given equivalently either by the classical Rankine–Hugoniot relation or the Rankine–Hugoniot relations just derived:

$$\frac{V_s^2}{a_{f1}^2} = \frac{\gamma+1}{2\gamma}\frac{p_f}{p_1} + \frac{\gamma-1}{2\gamma}, \tag{21}$$

$$\frac{V_s^2}{(a_e)_1^2} = \frac{\gamma_e+1}{2\gamma_e}\frac{p_2}{p_1} + \frac{\gamma_e-1}{2\gamma_e}, \tag{22}$$

where γ is the isentropic exponent of the vapour phase (i.e. ratio of the two specific heats) and a_{f1} is the upstream frozen speed of sound, given by

$$a_{f1} = (\gamma p_1/\rho_{g1})^{\frac{1}{2}}. \tag{23}$$

For a prescribed pressure ratio p_2/p_1, (21) and (22) together would specify the intermediate pressure p_f achieved just after the frozen shock. The pressure rises almost discontinuously (within a few mean free paths) from p_1 to p_f across the frozen shock and undergoes a further rise, in the relaxation zone through which the mixture attains equilibrium, to the downstream pressure p_2. If the vapour ahead of the shock was completely dry then one would expect from common sense that p_f should be

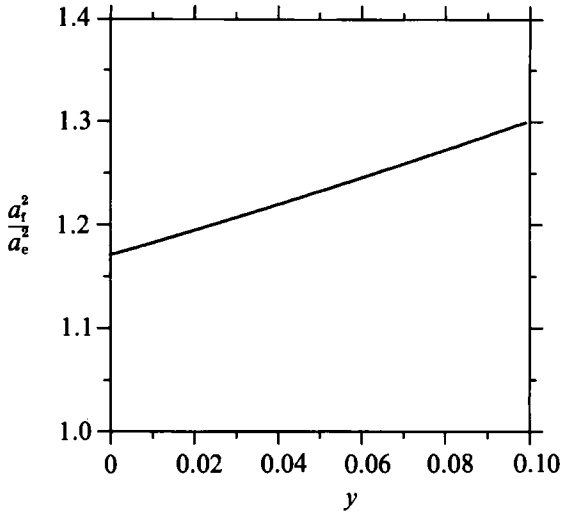

FIGURE 3. Variation of a_f^2/a_e^2 with wetness fraction; $p = 0.35$ bar.

equal to p_2 and (21) and (22) should become identical in the limit as $y_1 \to 0$, since without any droplets present there should not be any relaxation zone behind the frozen shock. That they do not become so is apparent from figure 3, which shows that the equilibrium sound speed a_e calculated from (18) does not coincide with the frozen speed a_f in the limit $y \to 0$, and therefore the shock speed V_s calculated from (21) and (22) would be different. Young & Guha (1991) have noted the previous notion of the occurrence of such a discontinuity in the speed of sound across the saturation line (as if the speed of sound on the saturation line depends on whether it is approached from the dry vapour or the wet vapour side) and have given an explanation for its apparent existence. Here we concentrate on the anomaly in the case of shock waves (in the sense that (22) is not only invalid in the case of $y_1 \to 0$ but also for higher values of y_1 up to a certain limit) and provide a solution for that problem.

5. Complete evaporation inside the relaxation zone

The key point in understanding the paradox is that, while deriving (22), we tacitly assumed that the vapour is wet and at equilibrium both upstream and downstream of the shock wave. If the imposed pressure ratio is too high, this may not be the case and complete evaporation of the droplets may take place inside the relaxation zone. In such a case, upstream of the shock wave the fluid is an equilibrium two-phase mixture whereas downstream of the shock it is single-phase vapour alone. (This problem does not arise in solid-particle-laden gas.) The downstream vapour-phase temperature is no longer the saturation temperature corresponding to the prevailing pressure and (22) is no longer valid.

In order to calculate the shock velocity when complete evaporation takes place, one has to write the basic conservation equations across the shock and solve them directly. Since the downstream wetness fraction y_2 is zero, it can be dropped from the equations:

continuity $$\rho_1 V_1 = (p_2/RT_2)\, V_2, \tag{24}$$

momentum $$p_1 + \rho_1 V_1^2 = p_2 + (p_2/RT_2)\, V_2^2, \tag{25}$$

energy $$c_p T_{s1} + \tfrac{1}{2}V_1^2 - y_1 h_{fg1} = c_p T_2 + \tfrac{1}{2}V_2^2. \tag{26}$$

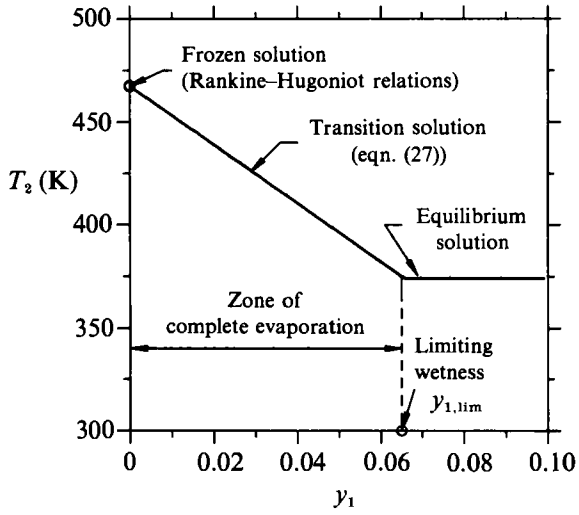

FIGURE 4. Variation of T_2 with y_1 for $p_1 = 0.35$ bar, $p_2/p_1 = 3.0$.

If the initial pressure p_1, initial wetness fraction y_1 and the pressure ratio p_2/p_1 are given then T_{s1} and ρ_{g1} become specified automatically by the Clausius–Clapeyron equation, (3), and the equation of state, (2), respectively. Equations (24), (25) and (26) can then be solved simultaneously for the three unknowns V_1, T_2 and V_2. It is to be noted that, since downstream of the shock the vapour is no longer wet, T_2 is not equal to T_{s2}. In this case it is possible to obtain an analytical solution (after algebraic manipulation) for the downstream temperature T_2 and the shock velocity V_1, given by

$$T_2 = \frac{T_{s1}\left(1+\frac{p_2-p_1}{p_1}\frac{\gamma-1}{2\gamma}\right)-\left(\frac{h_{fg1}}{c_p}+\frac{p_2-p_1}{p_1}\frac{\gamma-1}{2\gamma}T_{s1}\right)y_1}{\left(1-\frac{p_2-p_1}{p_2}\frac{\gamma-1}{2\gamma}\right)}, \tag{27}$$

$$V_1^2 = \frac{p_2-p_1}{\rho_1}\left(1-\rho_1\frac{RT_2}{p_2}\right)^{-1}. \tag{28}$$

Once T_2 and V_1 are found, V_2 can be calculated from (24).

It can be seen from (27) that for constant p_1 and for a fixed pressure ratio p_2/p_1, the downstream temperature T_2 decreases linearly with y_1. Equation (28) then shows that the shock velocity ($V_s = V_1$) also decreases with increasing upstream wetness fraction y_1. Figures 4 and 5 show the variation of downstream temperature and shock velocity respectively as a function of y_1, as predicted by (27) and (28), for $p_1 = 0.35$ bar and $p_2/p_1 = 3.0$ (with corresponding $T_{s1} = 347.9$ K, $\gamma = 1.32$ and $\gamma_e = 1.1274$). It is clear that if y_1 is set equal to zero in (27) and (28), the Rankine–Hugoniot relations for single-phase vapour are regained.

According to figures 4 and 5, as upstream wetness fraction y_1 is increased, keeping the pressure ratio fixed, both the downstream temperature and shock velocity decrease. They would continue to do so until the vapour downstream becomes just wet, i.e. vapour temperature just equals the saturation value corresponding to p_2. The limiting value of y_1 for the particular pressure ratio chosen ($p_2/p_1 = 3$), is $y_{1,\mathrm{lim}} \approx 0.065$. If y_1 is increased further, T_2 is no longer independent of p_2 ($T_2 = T_{s2}$) and (24)–(28) are no longer valid. y_2 must now be treated as a new variable and the

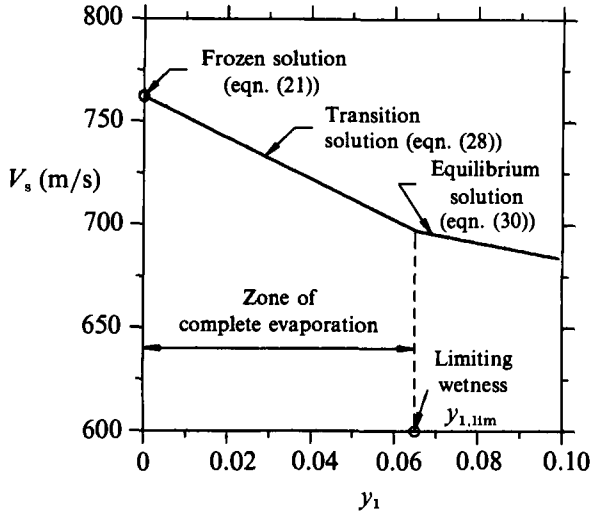

FIGURE 5. Variation of V_s with y_1 for $p_1 = 0.35$ bar, $p_2/p_1 = 3.0$.

original equations for an equilibrium shock ((1)–(7)) must be solved. For a prescribed pressure ratio (rather than specifying the upstream velocity V_1) an accurate closed-form analytical solution of the equations is possible (without introducing the approximate energy equation (14)) and is given by

$$y_2 = \frac{2c_p(T_{s2}-T_{s1})+2y_1 h_{fg1}-(p_2-p_1)/\rho_1-RT_{s2}(p_2-p_1)/p_2}{2h_{fg2}-RT_{s2}(p_2-p_1)/p_2}, \tag{29}$$

$$V_1^2 = ((p_2-p_1)/\rho_1)(1-(\rho_1(1-y_2)RT_{s2})/p_2)^{-1}. \tag{30}$$

All the quantities on the right-hand side of (29) being known, y_2 may be evaluated and then the upstream velocity V_1 may be calculated from (30). One can now assess the accuracy of the approximate equations (15)–(20) by comparing them with (29) and (30). (Equations (29) and (30) have to be solved iteratively for prescribed V_1.) Figure 6 shows such a comparison. The velocity or pressure calculated from the two sets of equations are virtually indistinguishable on the scale of the graph and hence only the net evaporation is plotted. It can be seen that the approximate equations work reasonably well until the strength of the shock is such that the mixture is close to complete evaporation.

Thus if $y_1 = 0$, the velocity of the shock is given by the frozen-shock relation, (21), with p_f replaced by p_2. If y_1 is greater than or equal to the limiting value $y_{1,\lim}$, for which downstream of the shock the vapour is wet, the velocity of the shock is given by the equilibrium relation, (30). For intermediate values of y_1, $0 \leqslant y_1 \leqslant y_{1,\lim}$, complete evaporation takes place inside the dispersed shock and the above theory, (28), shows that there is a continuous transition in the shock velocity from the frozen to the equilibrium value. Thus (28) becomes identical with the frozen-shock relation (21) in the limit $y_1 = 0$, and becomes identical with the equilibrium shock relation (30) in the limit $y_1 = y_{1,\lim}$. The discontinuity in the slope of the shock velocity at $y_1 = y_{1,\lim}$ (figure 5) is caused by the discontinuity of slope of various properties across the saturation line, for example of an isotherm on the Mollier diagram.

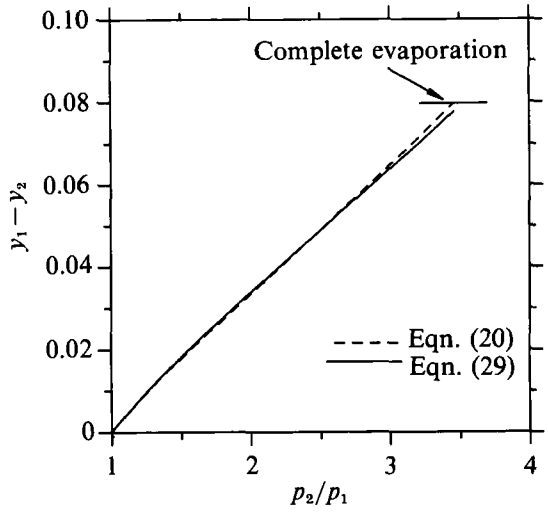

FIGURE 6. Comparison of approximate Rankine–Hugoniot relations with exact solution for $p_1 = 0.35$ bar, $y_1 = 0.08$.

6. Limiting wetness fraction

For different values of the pressure ratio p_2/p_1, the limiting wetness fraction $y_{1,\lim}$, below which complete evaporation takes place, is different. The appropriate limiting values can be found either by setting $T_2 = T_{s2}$ in (27) or setting $y_2 = 0$ in (29), and is given by

$$y_{1,\lim} = \frac{T_{s1}\left(\frac{p_2 - p_1}{p_1}R + 2c_p\right) - T_{s2}\left(2c_p - \frac{p_2 - p_1}{p_2}R\right)}{2h_{fg1} + \frac{p_2 - p_1}{p_1}RT_{s1}}, \tag{31}$$

which can be rewritten as

$$y_{1,\lim} \approx \frac{((\tilde{P}-1) + 2\gamma/(\gamma-1)) - \tilde{P}^{\tilde{H}}(2\gamma/(\gamma-1) - (\tilde{P}-1)/\tilde{P})}{2/\tilde{H} + \tilde{P} - 1}, \tag{32}$$

where $\tilde{P} = p_2/p_1$ and $\tilde{H} = RT_{s1}/h_{fg1}$.

Equation (32) shows that this limiting wetness fraction $y_{1,\lim}$ predominantly depends on the pressure ratio p_2/p_1 and is only a slowly varying function of the absolute level of upstream pressure p_1 (through $\tilde{H}$). Equation (31) is plotted in figure 7, which gives the variation of $y_{1,\lim}$ with pressure ratio p_2/p_1. The curve denotes the boundary line for complete drying. For shock conditions below the curve ($y_1 < y_{1,\lim}$), the downstream vapour is dry, whereas for shock conditions above the curve ($y_1 > y_{1,\lim}$), equilibrium exists both upstream and downstream of the shock.

7. Net evaporation inside a dispersed shock wave

If the upstream wetness fraction is higher than the limiting value $y_{1,\lim}$ for the same pressure ratio p_2/p_1, (29) shows that the net evaporation across the wave ($\Delta y = y_1 - y_2$) decreases with increasing upstream wetness fraction y_1. In figure 8 the

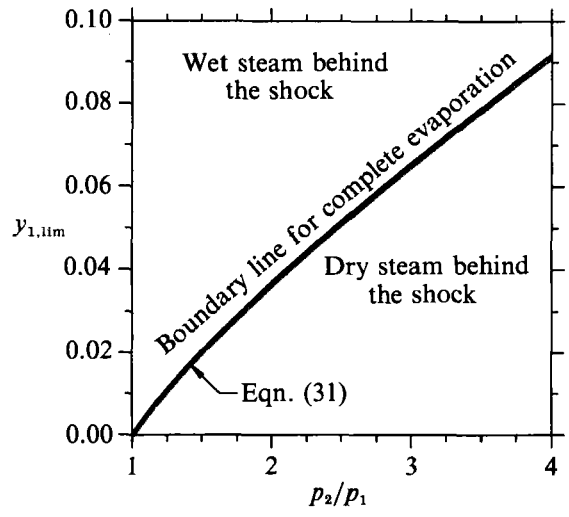

FIGURE 7. Variation of limiting wetness fraction with pressure ratio for shock waves in low-pressure steam.

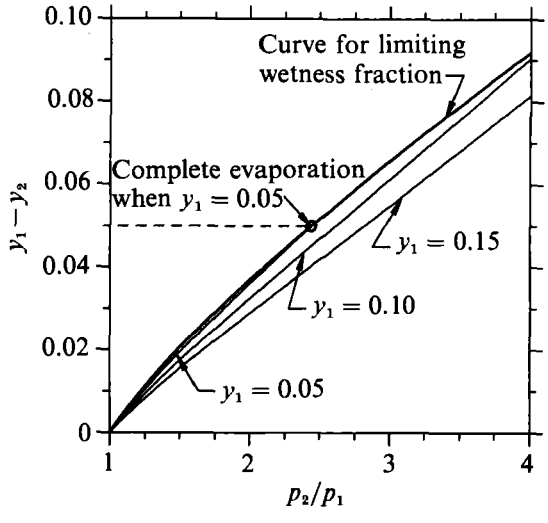

FIGURE 8. Variation of net evaporation with pressure ratio for shock waves in low-pressure steam.

net evaporation has been plotted against pressure ratio across the shock, for three different values of y_1. On the same graph, the limiting wetness fraction corresponding to the same pressure ratios is plotted. All the Δy *vs.* p_2/p_1 curves start from the origin, as the net evaporation is necessarily zero for a shock of zero strength. Also they must terminate on the limiting wetness fraction curve, as when the upstream wetness fraction equals the limiting value complete evaporation takes place. Figure 8 also shows that for any prescribed pressure ratio the net evaporation increases as y_1 is decreased, the maximum evaporation being $y_1 = y_{1,\lim}$.

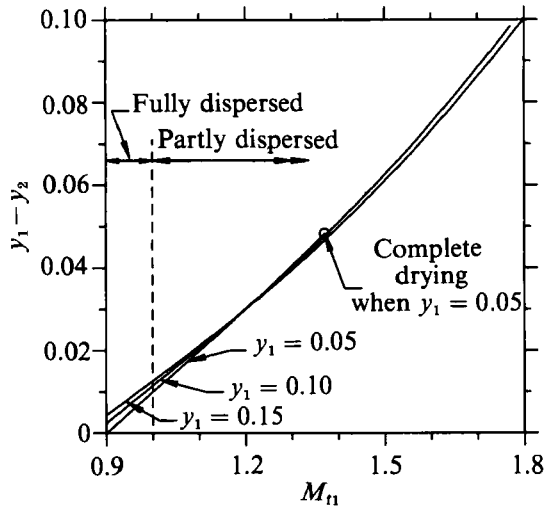

FIGURE 9. Variation of net evaporation with M_{f1} for shock waves in low-pressure steam.

The equation of state (2) together with (1) gives

$$(1-y_2)/(1-y_1) = (p_2/p_1)\,(T_{s1}/T_{s2})\,(\rho_1/\rho_2), \tag{33}$$

which can be rearranged as

$$\Delta y/(1-y_1) = f(p_2/p_1, \gamma_e), \tag{34}$$

since the approximate Rankine–Hugoniot relations show that all the quantities on the right-hand side of (33) are functions of p_2/p_1 and γ_e. Combining (1), (18), (21), (22) and (23), it is easy to show that

$$M_{f1}^2 = \frac{\gamma_e+1}{2\gamma}(1-y_1)\frac{p_2}{p_1} + \frac{\gamma_e-1}{2\gamma}(1-y_1). \tag{35}$$

Equation (35) shows that for moderate pressure ratios (so that the second term on the right-hand side of (35) may be removed) the upstream frozen Mach number M_{f1} is related to the pressure ratio by

$$\frac{p_2}{p_1} \approx \frac{2\gamma}{\gamma_e+1}\frac{M_{f1}^2}{(1-y_1)}. \tag{36}$$

Figure 8 shows that for moderate pressure ratio p_2/p_1 the function f in (34) is nearly linear. Equations (34) and (36) together then suggest that if the net evaporation Δy is plotted as a function of the upstream frozen Mach number, then curves for different y_1 would coincide. Figure 9 shows three such curves for three different upstream wetness fractions, calculated iteratively from the conservation equations ((5)–(7)). It is seen that they are reasonably close for moderate M_{f1}, the difference being higher for too high or too low values of M_{f1}. When M_{f1} is high, (14) is not a good approximation and so (34) and (36) are not accurate. When M_{f1} is low, the second term on the right-hand side of (35) is no longer negligible and hence (36) is again not valid. It is to be noted that the net evaporation is not zero when $M_{f1} = 1.0$ (as opposed to what has been shown in Konorski 1971), as fully dispersed shock waves

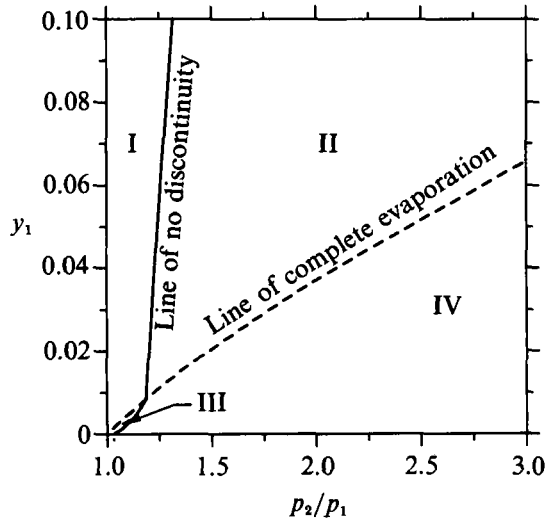

FIGURE 10. Phase diagram of different shock structures in low-pressure steam: I, equilibrium fully dispersed; II, equilibrium partly dispersed; III, fully dispersed with complete evaporation; IV, partly dispersed with complete evaporation.

may exist below that Mach number. The difference between M_{f1} and $(M_e)_1$ depends on the upstream wetness fraction y_1 and thus zero net evaporation occurs at different M_{f1} for different values of y_1, M_{f1} being lower for higher y_1. The limiting value of the upstream frozen Mach number below which normal shock waves cannot exist in wet vapour may be found by letting the pressure ratio p_2/p_1 tend to unity in (35), and is given by

$$M^2_{f1,\min} = (\gamma_e/\gamma)(1-y_1). \tag{37}$$

Equation (37) is valid until y_1 is too low. Depending on the strength of the small-amplitude wave p_2/p_1, there would be a small zone of y_1 (in the vicinity of $y_1 = 0$) through which $M^2_{f1,\min}$ would rise from γ_e/γ to the frozen requirement of unity.

8. Complete evaporation with or without a discontinuity

If the upstream frozen Mach number M_{f1} is greater than unity then a discontinuity appears in the flow field and a partly dispersed shock structure results. If, on the other hand, M_{f1} is less than unity but the equilibrium Mach number $(M_e)_1$ is greater than unity, a fully dispersed shock is obtained. Such an occurrence has been indicated in figure 9. However, what happens when complete evaporation takes place?

To investigate this problem, one can solve the conservation equations (5)–(7) iteratively for the upstream wetness fraction y_1, the inputs being a specified pressure ratio p_2/p_1 together with the limiting criterion for no frozen discontinuity in the flow field, i.e. $M_{f1} = 1$. If this calculation shows that the computed value of y_1 is less than the limiting wetness fraction $y_{1,\lim}$ for the same pressure ratio, then complete evaporation would take place and the calculation has to be repeated with the conservation equations (24)–(26) instead, the boundary conditions remaining the same. The results of such numerical calculations have been plotted in figure 10 as a solid line. Any condition towards the left of this line would mean that there is no frozen discontinuity in the flow field. On the same figure, the limiting wetness

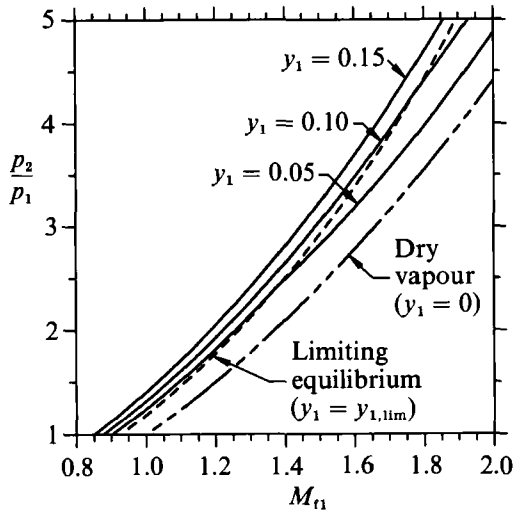

FIGURE 11. Variation of pressure ratio with upstream frozen Mach number for shock waves in low-pressure steam.

fraction *vs.* the pressure ratio is plotted, as a dotted line. Any condition below this line means that complete evaporation has taken place. Evidently the two curves divide the diagram into four regions. If the boundary conditions correspond to regions I and II, then equilibrium fully dispersed and equilibrium partly dispersed shock waves respectively are obtained. On the other hand region III corresponds to complete evaporation without any frozen discontinuity and region IV corresponds to complete evaporation with a frozen discontinuity present.

Although the line of no discontinuity, as shown in figure 10, was obtained by accurate numerical calculation, an approximately accurate expression representing a part of that line that separates region I from II can be obtained by setting $M_{f1} = 1.0$ in (35). The result is

$$y_1 = 1 - \left[\frac{\gamma/\gamma_e}{1 + ((\gamma_e + 1)/2\gamma_e)((p_2 - p_1)/p_1)}\right]. \tag{38}$$

There are two points worth mentioning. Firstly, (38) is not valid along the boundary between regions III and IV. The reason is obvious: the original equation (35) is not valid when complete evaporation takes place. Secondly, the tempting linearization of (38) in order to express y_1 as a linear function of p_2/p_1 (as figure 10 suggests) may lead to great inaccuracy in the computed value of y_1. As y_1 is calculated as the difference of two large numbers, a small percentage error in the value of the expression within the square bracket would result in a much higher relative error in y_1.

9. Conventional representation of jump conditions

It is conventional to represent the ratios of different flow variables between the two end states of a normal shock wave in an ideal gas as functions of the upstream Mach number. Following a similar convention, figure 11 plots the pressure ratio across normal shock waves in vapour–droplet flows as a function of upstream frozen

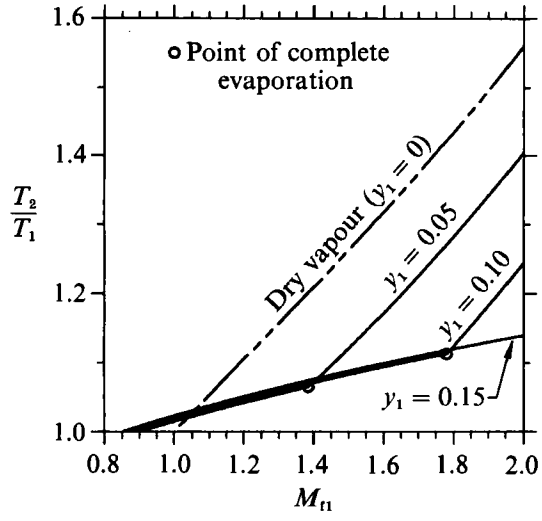

FIGURE 12. Variation of static temperature ratio with upstream frozen Mach number for shock waves in low-pressure steam.

Mach number M_{f1}. However, the curve is not unique in this case and depends on the wetness fraction y_1. For the same M_{f1}, higher y_1 leads to a higher pressure ratio. The Rankine–Hugoniot relation for dry vapour (ideal gas) has also been plotted in figure 11 for comparison. The pressure ratio achieved in this case is obviously always smaller than wet vapour, as pressure rises in the relaxation zone after the frozen shock. As another limiting case, the pressure ratio is plotted as a dotted line for shock waves such that the downstream vapour condition is marginally wet ($y_1 = y_{1,\mathrm{lim}}$). Whenever this line crosses other Rankine–Hugoniot plots (the solid lines), complete evaporation occurs. The dotted line thus divides each solid line into two segments where different sets of equations ((27)–(28) and (29)–(30)) hold and a discontinuity in the slope of the segments exists at the point of intersection. If two-phase equilibrium is maintained at both ends of the shock wave, (35) provides a simple but slightly approximate relation between upstream frozen Mach number and pressure ratio.

Figure 12 shows the static temperature ratio, again as a function of upstream frozen Mach number. For a shock wave where two-phase equilibrium persists at the downstream asymptote, the static temperature ratio is simply the ratio of the saturation temperatures corresponding to the upstream and downstream pressures. When complete evaporation takes place, the downstream temperature is independent of the pressure there and is given by (27). The static temperature ratio for the limiting case of dry vapour is also plotted on the same diagram.

The analysis in this paper depends on integral arguments. It relates the far upstream condition with the far downstream one, without any reference to what happens in between. On the other hand, if one is interested in the shock wave profile, one has to solve numerically the relevant differential equations (Guha & Young 1989). It is interesting to compare the asymptotic values of different variables obtained from such calculations, with the Rankine–Hugoniot relations obtained from the present integral analysis. Such a comparison demonstrates independent theoretical consistency.

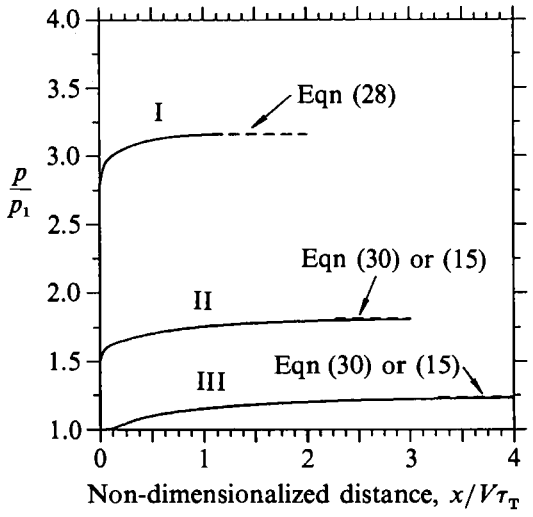

FIGURE 13. Comparison of asymptotic pressure profiles with generalized Rankine–Hugoniot equations: I, partly dispersed with complete evaporation ($p_1 = 0.35$ bar, $M_{f1} = 1.6$, $y_1 = 0.05$, $r_1 = 0.1$ μm); II, equilibrium partly dispersed ($p_1 = 0.35$ bar, $M_{f1} = 1.2$, $y_1 = 0.05$, $r_1 = 0.1$ μm); III, equilibrium fully dispersed ($p_1 = 0.35$ bar, $M_{f1} = 0.97$, $y_1 = 0.1$, $r_1 = 0.1$ μm).

Figure 13 shows three such comparisons, chosen to represent different types of shock waves: equilibrium partly dispersed, equilibrium fully dispersed and partly dispersed with complete evaporation. The ordinate is normalized by the upstream static pressure. There is a discontinuous wave front if the wave is partly dispersed. The abscissa is the distance normalized by $\tau_T V$, where V is the upstream velocity in the case of a fully dispersed wave or the velocity just after the frozen shock in the case of partly dispersed wave, and τ_T is the thermal relaxation time as defined in Guha & Young (1989). To obtain the wave profile one has to specify the radius of the droplets as well, which is taken to be 0.1 μm in all the examples. The origin on the abscissa corresponds to the position of the frozen shock for a partly dispersed wave and to an arbitrarily small perturbation for a fully dispersed wave. The dotted lines in the figure represent the Rankine–Hugoniot calculations. In the case of complete evaporation, (27) and (28) were used for this purpose. For the remaining two cases, final downstream pressures were calculated both by (15) and by (29) and (30) which give almost the same answer. It is noted that for all three cases the asymptotic values of the downstream pressure obtained by solving the differential equations agree well with the generalized Rankine–Hugoniot calculations.

10. Entropy rise through the shock wave

If the vapour is always dry, both upstream and downstream of the shock, then the entropy rise through the shock is simply

$$(s_2 - s_1)/c_v = \ln (p_2/p_1)\,(\rho_1/\rho_2)^{\gamma}, \tag{39}$$

where

$$\frac{\rho_2}{\rho_1} = \frac{1 + (\gamma+1)/(\gamma-1)\,(p_2/p_1)}{(\gamma+1)/(\gamma-1) + (p_2/p_1)}. \tag{40}$$

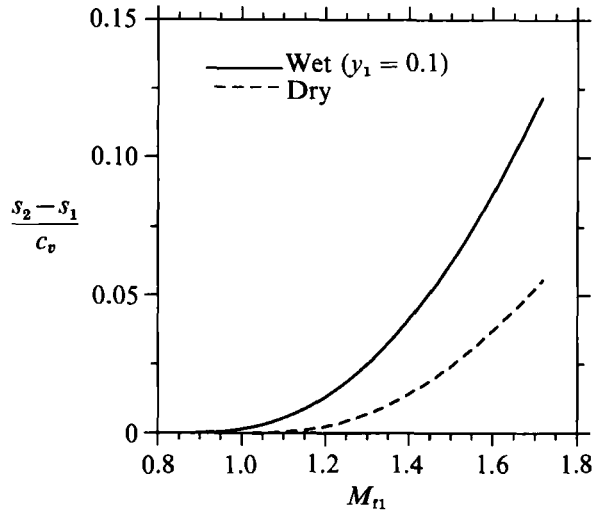

FIGURE 14. Entropy rise *vs.* upstream frozen Mach number for shock waves in low-pressure steam.

If the vapour is wet equilibrium both upstream and downstream of the shock, then the entropy rise can be calculated directly from

$$s_2 - s_1 = [(1-y_2)\,s_{g2} + y_2\,s_{l2}] - [(1-y_1)\,s_{g1} + y_1\,s_{l1}], \tag{41}$$

where the entropies s_{g2} and s_{l2} can be easily calculated once the downstream state has been determined from the jump conditions derived previously. In a partly dispersed shock wave there are two sources of entropy production: (i) that due to viscosity and thermal conductivity as in a normal shock wave in an ideal gas, and (ii) that due to different interphase transfer processes occurring in the relaxation zone following the frozen shock. (The liquid droplets pass through the frozen shock without any change of radius, temperature and velocity, and hence the two-phase mixture just after the frozen shock is out of equilibrium.) In a fully dispersed wave, the relaxation processes are solely responsible for the creation of entropy. In such waves, non-equilibrium variables such as velocity slip and vapour superheat grow to a maximum and then decrease continuously so that the downstream equilibrium state is reached.

It should be noted that in a normal shock wave in an ideal gas, although viscosity and thermal conductivity are responsible for the entropy production, they do not determine the total entropy rise across the shock wave. The total entropy rise is fixed by the integral conservation equations. Viscosity and thermal conductivity only determine the extent of the transition layer (normally a few mean free paths) through which such rise in entropy, fixed by Rankine–Hugoniot relations, would take place. Similarly, the total entropy rise through the relaxation zone in a dispersed shock wave is fixed by the conservation equations. Different relaxation times characterizing the relaxation processes would determine the distribution of such loss and hence the thickness of the dispersed shock wave (see the Appendix for further details).

The entropy rise for the different cases has been plotted in figure 14. As expected, for the same frozen Mach number, the entropy rise in the wet vapour is greater than that in the dry vapour owing to the presence of different non-equilibrium effects. For

example, for an upstream frozen Mach number of 1.7, the entropy rise in wet steam (with $y_1 = 0.1$) is more than double that in the dry vapour.

11. Conclusion

The approximate Rankine–Hugoniot relations ((15)–(20)) for a normal shock wave in wet vapour have been derived. (Like the conventional case, all the upstream conditions are assumed to be known, whereas downstream conditions are to be predicted.) For moderate pressure ratios, these relations can predict the downstream conditions with reasonable accuracy. The equations are valid for both partly and fully dispersed waves. However, they are not valid if complete evaporation occurs inside the dispersed shock wave. (Note that in the case of solid-particle-laden gas, similar equations with suitable γ are exact and hold unconditionally.)

If, instead of the upstream velocity, the pressure ratio across the shock is treated as an independent variable, then an exact closed-form analytical solution ((29) and (30)) of the conservation equations is possible (without requiring any approximate energy equation, e.g. (14)). This solution applies to partly and fully dispersed waves when the fluid remains an equilibrium two-phase mixture at both the upstream and downstream ends of the shock wave. However, if complete evaporation takes place inside the dispersed shock wave, the conservation equations yield a different set of jump conditions across the shock ((27) and (28)).

For a prescribed pressure ratio across the shock, an expression for the limiting upstream wetness fraction $y_{1,\mathrm{lim}}$, (31), has been formulated. If the actual upstream wetness fraction is less than this limiting value, complete evaporation takes place inside the dispersed shock. The analytical theory developed here (equation (28)) shows that, depending on the upstream wetness fraction, the shock velocity continuously varies from the frozen (equation (21)) to the equilibrium value ((22) or (30)). Equation (37) specifies the minimum frozen Mach number below which steady normal shock waves do not exist in vapour–droplet flow.

This study also shows that in addition to the usual types of partly and fully dispersed shock waves that exist in any general relaxation medium, there also exists a class of shock waves in wet vapour in which the two-phase relaxing medium reverts to a single-phase non-relaxing one. Depending on the pressure ratio attained and upstream wetness fraction, such shock waves may or may not involve a frozen discontinuity (figure 10). This peculiarity is a consequence of phase change in vapour–droplet mixtures.

The author is grateful to Dr J. B. Young for his helpful comments on the manuscript, and to Gonville & Caius College, Cambridge for awarding him a Research Fellowship.

Appendix. On the entropy production inside a shock wave

As a prelude to understanding how the integral equations can predict the entropy production inside a dispersed shock wave in vapour–droplet flow, we start with the one-dimensional Euler equations of motion for an ideal gas:

continuity	$\mathrm{d}(\rho V A) = 0,$	(A 1)
momentum	$\mathrm{d}A(p+\rho V^2) - p\mathrm{d}A = 0,$	(A 2)
energy	$\mathrm{d}(c_p T + \tfrac{1}{2}V^2) = 0,$	(A 3)

where A is the flow area. The above equations can be combined together to show $\mathrm{d}s = 0$; thus the process is isentropic. In fact the momentum and energy equations become equivalent in this case and one of them may be abandoned. However, if these equations are integrated between points 1 and 2, assuming the area remains constant, one obtains the shock relations:

continuity	$\rho_1 V_1 = \rho_2 V_2,$	(A 4)
momentum	$p_1+\rho_1 V_1^2 = p_2+\rho_2 V_2^2,$	(A 5)
energy	$c_p T_1+\frac{1}{2}V_1^2 = c_p T_2+\frac{1}{2}V_2^2.$	(A 6)

The momentum and energy equations in the integrated form are no longer identical (except in the trivial case when all upstream conditions are same as downstream ones) and these apparently 'inviscid' equations predict a fixed entropy generation across the shock wave.

In order to solve this apparent paradox, one realizes that there must be some real physical mechanism in the flow to produce the dissipation which the equations predict and that no real discontinuities can exist. In fact across such high gradients of velocity and temperature, viscosity and thermal conductivity, however small they might be, come into play and give rise to a transition layer of finite thickness over which the changes in flow properties take place. It is possible to analyse the flow structure within this transition layer by using the Navier–Stokes equations. However, it has been argued that the thickness of the transition zone is comparable to the mean free path and hence continuum fluid mechanics should not be applied there. Suggestions have been made rather to apply directly the Boltzmann equation from kinetic theory. Despite the difficulties, Navier–Stokes analysis should give a qualitatively correct physical picture (Courant & Freidrichs 1948) in which we are interested here. The four laws then reduce to

continuity	$(\rho V)_x = 0,$	(A 7)
momentum	$(p+\rho V^2-\mu V_x)_x = 0,$	(A 8)
energy	$[\rho V(h+\frac{1}{2}V^2)-\mu V V_x-\lambda T_x]_x = 0,$	(A 9)
entropy	$\rho V T s_x = \mu V_x^2+(\lambda T_x)_x,$	(A 10)

where the subscript x refers to differentiation with respect to x.

Obviously (A 7)–(A 9) can be integrated across the shock, the far upstream and downstream conditions being such that the derivatives of all flow variables are vanishingly small. Otherwise one may consider what happens in the limit $\mu \to 0$, $\lambda \to 0$ and then let the point 1 approach 2. Such integrations would reproduce equations (A 4)–(A 6) which were also obtained by integrating Euler's equations. However, integration of the entropy equation (A 10) gives

$$\rho_1 V_1(s_2-s_1) = \int_1^2 \mu \frac{V_x^2}{T}\,\mathrm{d}x+\int_1^2 \lambda \frac{T_x^2}{T^2}\,\mathrm{d}x+\left[\frac{\lambda T_x}{T}\right]_1^2. \tag{A 11}$$

Although the last term on the right-hand side of (A 11) tends to zero, the other two terms involve integrals over an interval within which T_x^2 and V_x^2 become very large in the limiting process. They always make a positive contribution and are responsible for the increase in entropy. Thus, although the differential form of the conservation equations, (A 1)–(A 3), represent an isentropic process, the integral forms, (A 4)–(A 6), are valid across a normal shock wave.

Similarly, for a vapour–droplet mixture, the normal shock conditions, (5)–(7), may

be thought of as being derived by integrating differential equations of motion which are valid for an inviscid, equilibrium two-phase mixture (hence isentropic). On the other hand, one could write a general set of equations for a vapour–droplet mixture that would be valid inside the relaxation zone of a shock wave (Guha & Young 1989):

$$\text{continuity} \qquad \mathrm{d}[\rho_g V_g + y/(1-y)\,\rho_g V_l] = 0, \tag{A 12}$$

$$\text{momentum} \qquad \mathrm{d}[p + \rho_g V_g^2 + y/(1-y)\,\rho_g V_l^2] = 0, \tag{A 13}$$

$$\text{energy} \qquad \mathrm{d}[\rho_g V_g(h_g + \tfrac{1}{2}V_g^2) + y/(1-y)\,\rho_g V_l(h_l + \tfrac{1}{2}V_l^2)] = 0, \tag{A 14}$$

where the subscript l represents liquid phase. In order to close the system of equations, the above three equations are supplemented by the equation of state of the vapour phase and three equations characterizing the interphase transfer of mass, momentum and energy. If (A 12)–(A 14) are integrated between state points 1 and 2, where the vapour droplet mixture is in inertial and thermodynamic equilibrium, (5)–(7) are regained. It should be noted that the integration could be performed without any direct reference to the interphase transfer processes. Thus explicit inclusion of the non-equilibrium, relaxation processes in the differential equations has no effect on the integral conservation equations. However, the mixture is not at equilibrium inside the relaxation zone. Hence, entropy is created continuously because of the drag originated from velocity slip and the irreversible heat and mass transfer because of phase change.

The general form of the equation for the production of entropy in the relaxation zone can be deduced from (A 12)–(A 14) but is complicated. The qualitative feeling can, however, be obtained by assuming that the relaxation takes place in two distinct stages (Young & Guha 1991). In the first stage inertial equilibration takes place with frozen heat transfer and in the second stage the temperature equalization takes place. It can be shown that the entropy increase for the first process is given by

$$\frac{\mathrm{d}s_I}{\mathrm{d}x} \approx \frac{y}{V_l T_s}\frac{\Delta V^2}{\tau_I} \tag{A 15}$$

and that due to the second stage is

$$\frac{\mathrm{d}s_T}{\mathrm{d}x} \approx \frac{(1-y)\,c_p}{V_g T_s^2}\frac{\Delta T^2}{\tau_T}, \tag{A 16}$$

where $\Delta V = V_g - V_l$ and $\Delta T = T_s - T_g$ are the velocity slip and the vapour subcooling respectively. τ_I and τ_T are the inertial and thermal relaxation times as defined in Guha & Young (1989). Inside the relaxation zone of a shock wave the vapour is superheated and ΔT is negative.

Both equations (A 15) and (A 16) show that the change in entropy is proportional to the square of the non-equilibrium variables and hence entropy always increases in an infinitesimal change due to relaxation process. When equations (A 15) and (A 16) are integrated across the relaxation zone and then added together, this accounts for the contribution of the relaxation processes in the overall rise in entropy as predicted by the generalized Rankine–Hugoniot relations (entropy increases across the frozen shock in a partly dispersed wave because of viscous dissipation and thermal conduction).

REFERENCES

BECKER, E. 1970 Relaxation effects in gas dynamics. *Aeronaut. J.* **74**, 736–748.

COURANT, R. & FRIEDRICHS, K. O. 1948 *Supersonic Flow and Shock Waves.* Interscience.

GOOSENS, H. W. J., CLEIJNE, J. W., SMOLDERS, H. J. & DONGEN, M. E. H. VAN 1988 Shock wave induced evaporation of water droplets in a gas-droplet mixture. *Exp. Fluids* **6**, 561–568.

GUHA, A. 1991 The physics of relaxation processes and of stationary and non-stationary shock waves in vapour-droplet flows. *Presented at 4th Intl Symp. on Transport Phenomena in Heat and Mass Transfer, ISTP – 4, Sydney, 14–19 July* (ed. J. Reizes). Hemisphere (to appear).

GUHA, A. 1992 Structure of partly dispersed normal shock waves in vapour-droplet flows. *Phys. Fluids* A (in press).

GUHA, A. & YOUNG, J. B. 1989 Stationary and moving normal shock waves in wet steam. In *Adiabatic Waves in Liquid–Vapour Systems* (ed. G. E. A. Meier & P. A. Thompson), pp. 159–170. Springer.

GUHA, A. & YOUNG, J. B. 1991 Time-marching prediction of unsteady condensation phenomena due to supercritical heat addition. *Proc. Conf. Turbomachinery: Latest Developments in a Changing Scene, London, IMechE Paper* C423/057, pp. 167–177.

JACKSON, R. & DAVIDSON, B. J. 1983 An equation set for non-equilibrium two-phase flow, and an analysis of some aspects of choking, acoustic propagation, and losses in low pressure wet steam. *Intl J. Multiphase Flow* **9**, 491–510.

JOHANNESEN, N. H., ZIENKIEWICZ, H. K., BLYTHE, P. A. & GERRARD, J. H. 1962 Experimental and theoretical analysis of vibrational relaxation regions in carbon dioxide. *J. Fluid Mech.* **13**, 213–224.

KONORSKI, A. 1971 Shock waves in wet steam flow. *PIMP (Trans. Inst. Fluid Flow Machinery, Poland)* **57**, 101–109.

MARBLE, F. E. 1969 Some gas dynamic problems in the flow of condensing vapours. *Astronautica Acta* **14**, 585–614.

NAYFEH, A. H. 1966 Shock-wave structure in a gas containing ablating particles. *Phys. Fluids* **12**, 2351–2356.

ROTH, P. & FISCHER, R. 1985 An experimental shock wave study of aerosol droplet evaporation in the transition regime. *Phys. Fluids* **28**, 1665–1672.

RUDINGER, G. 1964 Some properties of shock relaxation in gas flows carrying small particles. *Phys. Fluids* **7**, 658–663.

YOUNG, J. B. & GUHA, A. 1991 Normal shock wave structure in two-phase vapour droplet flows. *J. Fluid Mech.* **228**, 243–274.